Fall 11-29-2022

Prototyping a Novel Mach-Zehnder Interferometer with Acousto-Optic Modulators

Jon Mills
Eastern Kentucky University, jon_mills99@mymail.eku.edu

EASTERN KENTUCKY UNIVERSITY

Prototyping a Novel Mach-Zehnder Interferometer with Acousto-Optic Modulators

Honors Thesis

Submitted

in Partial Fulfillment

of the

Requirements of HON 420

Fall 2022

By

Jon Mills

Mentor

Dr. Thomas Jarvis

Department of Physics, Geosciences, and Astronomy

Prototyping a Novel Mach-Zehnder Interferometer with Acousto-Optic Modulators

Jon Mills

Thomas Jarvis

Department of Physics, Geosciences, and Astronomy

The Mach-Zehnder interferometer (MZI) is a ubiquitous optical tool that has been used for decades in a variety of applications. However, its design has undergone little to no updating throughout this time, and it remains expensive to install and difficult to scale. This limitation is due to the need for precise translation stages and mirrors to carefully direct the beams. Because of this, we propose the use of acousto-optic devices to simplify the design of the MZI and make it more accessible and scalable. By using acousto-optic modulators (AOMs), it is possible to direct the beams using radio frequency (RF) signals, produced and controlled by a computer, to create a delay between two collinear pulses. By altering the delay between these pulses, it should be possible to create precise interference that can be used in place of a conventional MZI. Some potential issues with this design are the interference from intermodulation modes created by the AOMs and the loss of diffraction efficiency in the AOMs due to signal modulation. In this experiment, we have setup our design of the AOM MZI using a double-pass multiplexed AOM system, and we discuss our methods of evaluating this design and measuring the delay created between the pulses. Although the delay measurement is a work in progress, we provide positive results for the diffraction efficiency of the AOM setup.

Keywords and Phrases: Interferometry, Mach Zehnder Interferometer, Acousto-optics, acousto-optic modulators, optics, pulse shaping, interference

Table of Contents

List of Figures

Acknowledgements

I would like to thank my mentor, Dr. Thomas Jarvis of the Department of Physics, Geosciences, and Astronomy, for providing me with the necessary guidance to bring his idea to the laboratory. This process has required a great deal of patience, determination, and wrench-turning. Additionally, I would like to thank the Eastern Kentucky University Honors Program for their guidance in completing this thesis.

Prototyping a Novel Mach-Zehnder Interferometer with Acousto-Optic Modulators

I. Background and Motivation

A. Fundamentals of Optics

The study of the interactions of light with physical systems, referred to as optics, allows for a precise understanding of nature. Light can be described as organized disturbances, or waves, which propagate through an electromagnetic field. These waves are produced by accelerating charges in space, such as excited electrons or energetic protons. These waves possess characteristics based on their interactions with the environment: frequency (or wavelength), amplitude, and phase (Figure 1). The frequency and wavelength of a wave describe how many oscillations of the wave pass by a certain point in a given amount of time. These values can also determine the speed or energy of a wave. The amplitude represents the intensity of the wave, and the phase describes the relative location or timing of the wave [1][2]. By observing these characteristics, we can draw conclusions about the previous interactions that the light has undergone. For example, the human visual system uses the wavelength, intensity, and phase of light that has been reflected off our surroundings to form an image of those surroundings; the wavelength is interpreted as color, and the intensity and phase determine the brightness. Similarly, any experimental light detection systems use these characteristics to provide

data about the experiment. In short, by studying the information carried by light, is possible to draw conclusions about the previous interactions of the light.

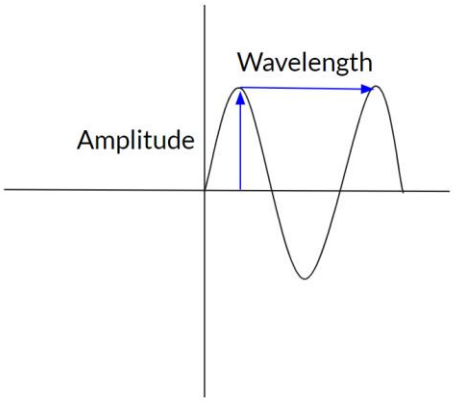

Figure 1: An example of the characteristics of light waves.

Of the characteristics of light previously described, our research will focus primarily on the phase. The study of how light's phase determines its interactions is known as interferometry. When light waves of the same phase interact, the amplitudes of the waves add together, and they are said to interfere constructively. When light waves of phases that differ by half a wavelength interact, their amplitudes subtract from each other, and they are said to interfere destructively (Figure 2). However, most interactions are more complex than these two ideal scenarios, and thus require a more complicated system of observation to determine their interference [2][3]. In order to utilize this phenomenon of interference in an experiment, scientists often use tools known as interferometers. These tools use mirrors and beam-splitters to separate light into separate beams, then recombine these beams after some interactions. The interference pattern in the subsequent signal can then be used to draw conclusions about the previous interactions. For example, interferometric spectroscopy uses a laser to determine the chemical composition of a gas

according to how it affects the beam's interference pattern. There are many different types of interferometers, but our research will focus on the Mach Zehnder Interferometer.

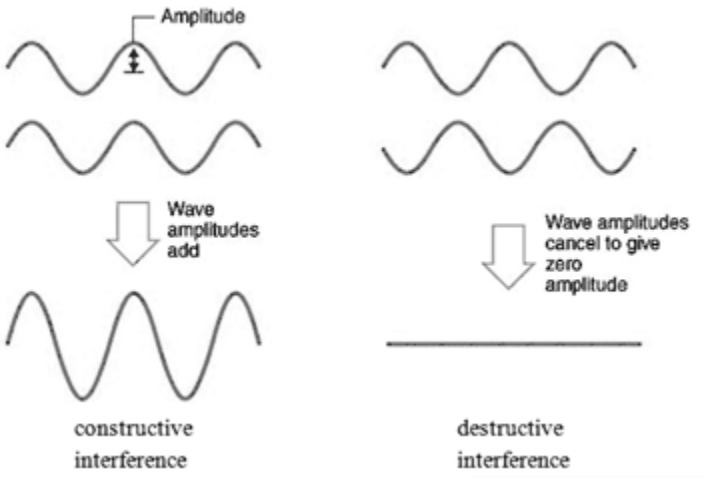

Figure 2: Demonstrations of constructive/destructive interference in waves [21].

B. The Mach-Zehnder Interferometer

The Mach Zehnder interferometer uses a beam splitter to separate the incoming light into two beams, before using two mirrors to recombine the beams with another beam splitter (Figure 3). This design allows every beam path to only be traversed once, and the phase shift between the recombined beams can be altered by either adding a sample (such as a gas in spectroscopy) in one beam path or additional mirrors on a translation stage [4][5]. This simple, adaptable design has made the Mach Zehnder interferometer a popular choice in optics experiments for well over a century. However, the design does have limitations. The greatest limitation is the need for very precise changes in the mirror positioning - on the order of nanometers. This requires the use of expensive translation stages, which can often be unattainable by low- to mid-budget optics labs. Also, this limitation makes it much harder to scale up the design to add more

than one beam path with independent phase and delay, as this requires yet another stage. Additionally, the alignment of the stages and mirrors also makes this design very limited—any vibrations or disturbances can ruin the alignment, making this design useless for an interferometer being used in rigorous applications i.e., for satellite research. However, an acousto-optic design would allow for the components to be set in place using epoxy for a permanent alignment. It is for these reasons that we will attempt to create a novel design of this interferometer using different components to make the alignment and phase shifting much easier, and the tool more useful for various experimental applications.

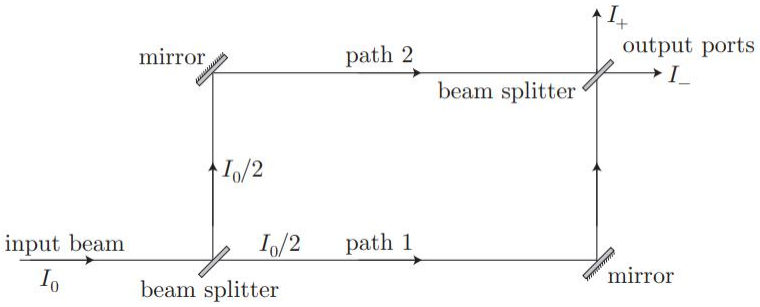

Figure 3: A diagram of the conventional MZI design [2].

C. Acousto-Optics and Acousto-Optic Modulators

The goal of our research is to redesign the Mach Zehnder interferometer to make the tool more accessible and scalable. To accomplish this, we will investigate the use of multiplexed acousto-optic modulators (AOMs) [6][7] to split a beam into two diffracted modes whose angles of diffraction can easily be modulated using computer-controlled direct digital synthesis radio frequency (DDS RF) sources (Figures 4 & 5). The capability of multiplexed AOMs to independently drive the frequency of multiple excitation sources

has already been investigated by Jarvis [6], but our work will build on these results by investigating their potential to precisely change the diffractive angle of multiple modes without compromising the diffraction efficiency. Also, we will investigate the use of nonlinear lock-in amplification measurement techniques to clarify the interferometric data [8] [9].

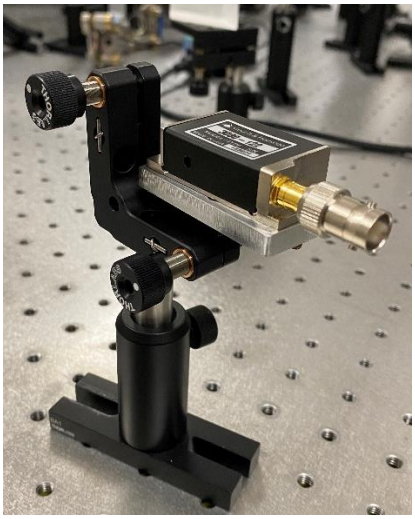

Figure 4: An AOM in our lab.

Figure 5: The DDS systems used in our experiment.

AOMs operate under the principles of acousto-optics, or the study of the interactions between light and sound waves. In their groundbreaking paper on acousto-optics, Debye and Sears reported the ability of supersonic waves, or high frequency RF signals, to predictably scatter light [10]. Theoretically, this interaction model can be simplified to largely resemble that of Bragg scattering, the prototypical model for understanding a broad range of scattering processes involving wavelike phenomena and periodic structures (Figure 6) [11][12]. Upon the development of lasers in the 1960s, the potential

for acousto-optics to be utilized in optical experiments increased drastically [13], and many new applications were created. An important example among these new applications included the AOM, which consists of a crystal (tellurium in the case of our research) attached to a piezo transducer (Figure 7). When an RF signal is sent to the piezo transducer, it causes the transducer to oscillate at a high frequency, which then mechanically oscillates the crystal in the form of an acoustic wave. This wave creates stress and strain within the atomic structure of the crystal and causes the light passing through the crystal to be diffracted (Figure 8). 6) The exact nature of this diffraction process may be best described as a Bragg or Raman-Nath process, but most aspects of acousto-optic phenomena are usually explained in terms of Bragg diffraction for simplicity. The efficiency of this diffraction process is proportional to the wavelength of the beam, as well as the frequency of the RF signal and to the amplitude of the acoustic vibrations launched into the acousto-optic medium by the transducer [11]. Because the beam diffraction is dependent on the RF signal, the modulation of the beam diffraction angle, power, or frequency can be controlled easily via the RF synthesis technology. For our experiment, we will use the LabView programming environment to automate the RF controls by adjusting the frequency and power level of the signal. By modulating the frequency of the RF signal with constant power, we can precisely adjust the diffraction angle of the resultant modes. Therefore, it should be possible to create an interferometer geometry in which modulating the RF frequency changes the difference in path length between two beams, and thus creates a measurable phase shift (Figure 9). This result would bypass the need for expensive translation stages and increase the scalability of the interferometer design.

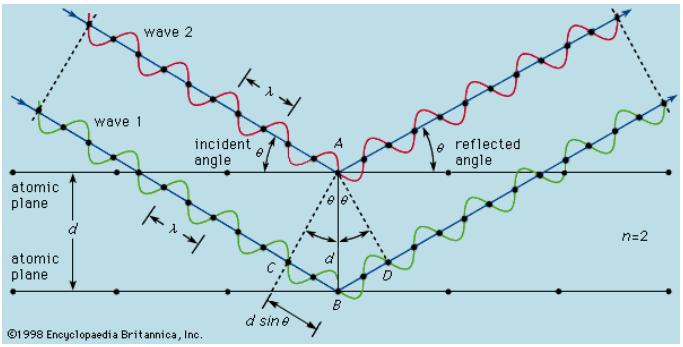

Figure 6: A diagram of Bragg diffraction in a crystal for two light rays [22].

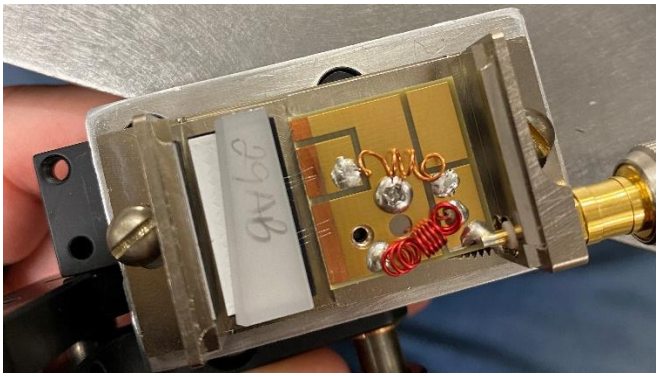

Figure 7: The interior of an AOM in our lab: shows the electronics and the piezo-transducer connected to the TeO2 crystal by the faintly visible wires.

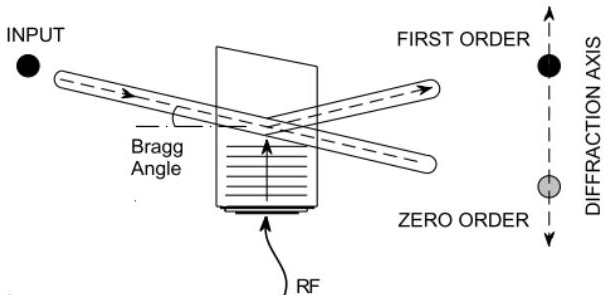

Figure 8: A simple schematic showing the deflection of a laser beam by a sound-wave in an AOM [23].

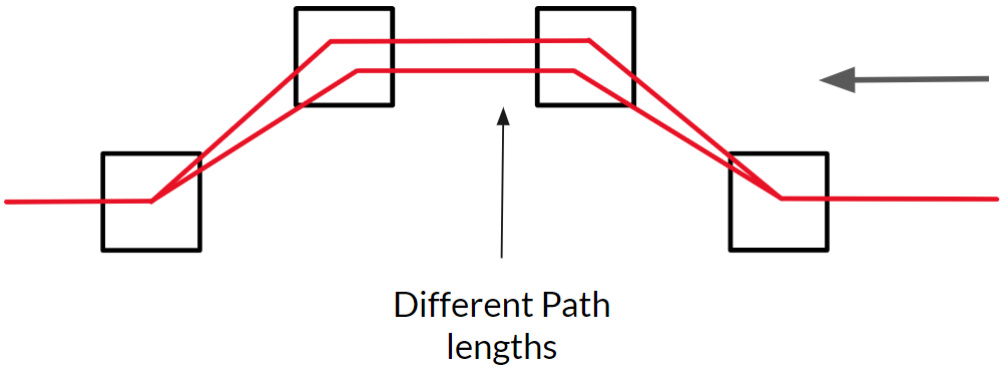

Figure 9: The preliminary design for our AOM MZI, with the boxes representing the AOMs.

To test the potential for using AOMs to construct a Mach Zehnder Interferometer, we must first test the use of multiplexed AOMs to create multiple diffracted modes. A multiplexed AOM uses additive RF signals to produce multiple diffracted modes rather than just a single signal. However, it is known that this process is nonlinear, and results in the diffraction of intermodulation modes – additional diffracted beams – that may add noise pulses to our desired pulse train. Also, by modulating the frequency of the RF

signal, the Bragg angle will also be modulated, and thus some diffraction efficiency may be lost. In order to determine the magnitude of the effect of these potential barriers, we will conduct experiments using multiplexed AOMs and analyze the resultant signals. To detect the weak signals that will be generated by our diagnostics, lock-in amplification methods will be used to suppress noise and integrate a greater intensity signal. This method uses a separate reference signal which is matched to the modulation frequency of the AOMs, to amplify a signal modulated at the frequency of interest.

On the conclusion of these tests, we will provide a unique result for the potential for multiplexed AOMs to be used to create an affordable, scalable Mach Zehnder interferometer. Using DDS RF technology to send an additive RF signal to an AOM, we will attempt to produce multiple diffracted modes which can easily be modulated using LabView. To analyze the interference of these modes, we will use lock-in amplification to filter out systematic noise and nonlinear 2 photon absorption to measure the signal. If successful, this result will lead to the development of a tool that can be used by more experimentalists to push the boundaries of discovery even further.

II. Experimental Setup

Throughout the evolution of this experiment, we used several variations of each component. The experimental configuration can be broken down into multiple parts: the RF synthesis and control circuit; the optical setup leading up to the pulseshaper; the AOM pulseshaper configuration; the pulsetrain measurement system; and the nonlinear detection system. These designs were created to fit into an existing optical table setup consisting of multiple other experiments, which would presumably be common to most optics labs attempting to implement this device. While the bulk of the external

components take up more space in this preliminary design, the most important parts of the pulseshaper – the AOMs, polarizing beam splitter, and retroreflecting mirror – take up a relatively small footprint on the table. The following sections will elaborate on the processes of optimizing the different component systems and the specifics of their final designs.

A. Radio Frequency Synthesis

To provide the necessary signals to drive the interferometers, we developed a system of RF components capable of producing precisely controlled signals, combining these signals, amplifying them, and then splitting them to send to multiple AOMs. The production of these signals was driven by a direct digital synthesis board (DDS) contained within the Novatech 409B RF synthesizer. The DDS board allows for the production of multiple independent frequency channels controlled simply by digital commands [14]. The Novatech synthesizer is controlled via serial commands, but thanks to the work of a previous student, I was able to use a premade serial command graphical user interface program in LabView to easily control the DDS by changing the frequency and power levels on a simple input VI. This VI initialized the communication with the DDS, converted the frequency and power level inputs to serial commands, and presented the serial output as a string. This made controlling the AOM diffraction as simple as changing a few numbers in a GUI.

For combining the different frequency channels and splitting them between the two AOMs, two different methods were tested. For the first method, I used a nonlinear mixer from Minicircuits [15] to combine the two frequencies, with one signal used as the local oscillator (LO) and the other used as the radio frequency (RF) signal. The

modulated signal is then output as the intermediate frequency (IF) and consists of a mixture of the sum and difference of the two input signals as can be shown through the use of some trigonometric identities. In our application, using a mixer allows for the modulation of the frequency independent of the other signal characteristics [15]. For the pulse shaping interferometer, the use of a mixer had several benefits. Because the output signal is dependent on the combination of the LO and RF input signals, and not just a linear combination of the two, it was possible to set a constant RF signal and only modify the LO signal. This made our diffraction geometry much more symmetric, since by changing one signal we could affect the two diffracted modes in the same way. However, this method also had its detriments which lead to the use of another component in the final design. In order to produce two identical signals, which are necessary to produce colinear diffracted modes, we had to send an LO signal with a frequency of 0 and an RF signal at our desired diffraction frequency (~80MHz). Due to the nonlinearity of the signal mixer, which does not function well below a low-frequency cut-off limit, this led to the production of an 80MHz signal with a drastically decreased power level, and therefore very low diffraction efficiency.

It was for this reason that we decided to instead use a frequency combiner/splitter component from Minicircuits (Figure 10). These devices add the frequencies of the input signals and produce an output at the power level that is the sum of the input power levels. When power is applied in reverse, they can act as a splitter that divides the input into two output signals with the same frequency and half the power level [16]. Because of this simplicity, it was simple to incorporate these into the circuit for both the combination of the different frequencies and the division of the amplified signal between the two AOMs.

However, this setup lacked the symmetry of the mixer design and required that both input frequencies be modulated dependently to control diffraction. Therefore, to produce the same path length for the pulses, each channel must have the same frequency, such as 80MHz, and to adjust the path length the frequencies must be changed by the same magnitude in opposite directions: 85MHz and 75MHz, for example, to a first approximation – the actual geometry of the diffraction is not strictly linear in the frequency of the applied RF signal, but it is close to it due to a small angle approximation. In this case, the small angle of diffraction arises due to the relatively miniscule momentum carried by a phonon, the quantized quasi-particle that carries an acoustic wave, compared to that carried by a photon, the particle interpretation of a light wave. However, this slight inconvenience in the operation was warranted to achieve a functional design at all frequency differences.

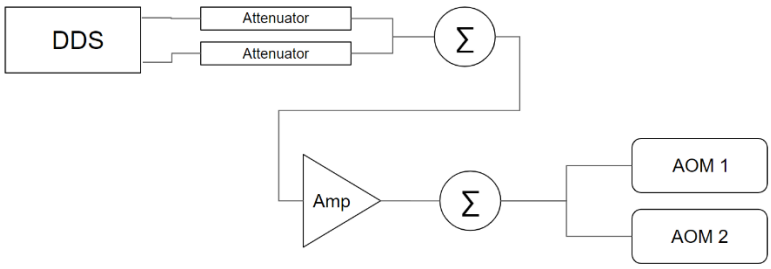

Figure 10: Our finalized multiplexing RF circuit Diagram.

In addition to combining and splitting the two signals, our RF circuit also needed to attenuate and amplify the signals. In our circuit, we used 2 10db Minicircuits attenuators for each channel, resulting in a total power attenuation of 20db per channel. This corresponds to a power reduction of roughly 10^{-2}. These attenuators were attached directly to the DDS output ports and were therefore the first components after synthesis.

Our reason for doing this is to preserve the linearity of the signal amplification and the lifetime of the amplifier. Although most amplifiers are rated for a relatively wide range of input power levels, the linearity of the output signal tends to decline as the maximum power level is approached. As such, we used the attenuators to ensure the power level of the input signal was sufficiently low before reaching the amplifier. The amplifier used was also from Minicircuits and featured a nominal power gain of 50 db (10^5). Since our AOMs displayed maximum diffraction efficiency at an RMS power of about 1 watt, this meant that our input power level at the amplifier needed to be about .01 mW for a single AOM, or double that for two AOMs. This amplifier was rated for a maximum input power of 3dbm, or 0.5 mW, so our input power at the amplifier was about 4% of the maximum power rating. With that being said, we still saw issues with the linearity of our output signal from the amplifier, as can be seen in the graph in figure 11 of output RMS power vs input RMS power. We are not sure about the cause of this issue, outside of the fact that there may be some discrepancy in the reliability of our amplifier. However, with careful compensation in the power level choice when operating the AOMs, this can be overlooked.

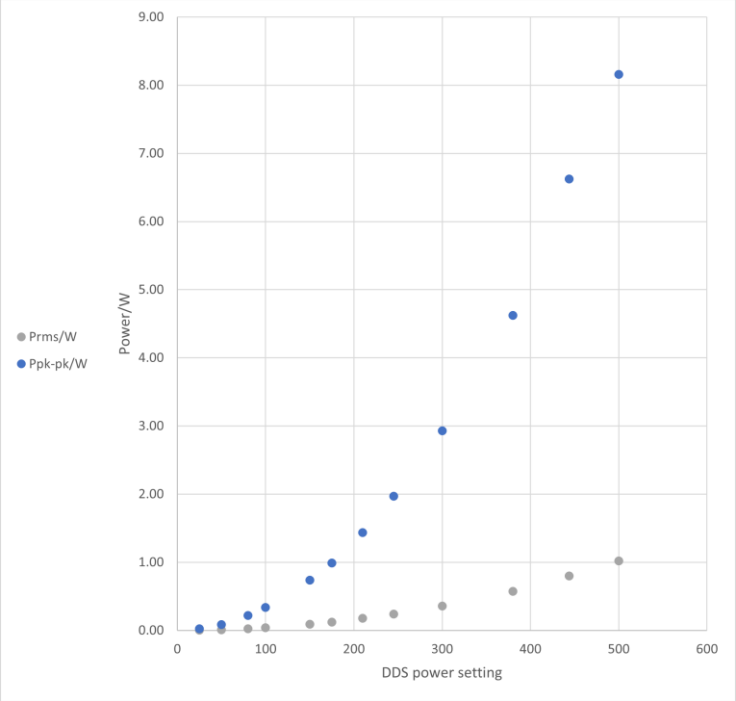

Figure 11: A graph showing the nonlinearity of the output power level from our amplifier as a function of the DDS power level setting.

B. AOM Testing

When it came time to test the AOMs, we went through multiple stages of testing before assembling the final design. These included testing a single AOM with a red HeNe laser, testing an AOM with the ultrafast Titanium:Sapphire, and then testing the single and double multiplexed AOMs with the Titanium:sapphire. For the HeNe test, we found that we were unable to get a sufficient diffraction efficiency into the first mode. This could be because the beam waist wasn't small enough, and because our beam was diverging too quickly. This would cause a significant amount of the light to enter at an angle different than the Bragg angle, and therefore diminish the diffraction efficiency. To attempt to resolve this issue, we used a Keplerian telescope [17] to narrow and recollimate the

beam, but this attempt was unsuccessful. We could not get a diffraction efficiency higher than a couple percent of the original power.

Following this, we moved to the more precise femtosecond Titanium:sapphire laser, tunable from 690-1050nm. While this laser may seem advanced for an application focusing on accessibility, it is important to note that this laser is by no means required to make this design work. However, according to Hardin, Mills, et al. [18], the prevalence of turnkey femtosecond lasers in undergraduate lab settings seems to be increasing due to their accessibility compared to other laser systems. Nevertheless, this test also seemed to yield the same result as with the HeNe, until we realized that the optimal RF power level specified for the AOM was in terms of the RMS power, rather than the power related to the peak-peak voltage. This discrepancy came about because the datasheet for the AOMs failed to specify is the rated power level was for peak-to-peak or RMS voltage, so we decided to use the peak-to-peak first to prevent damaging the AOMs with too much RF power. After accounting for this discrepancy (increasing the power level by a factor of ~2.8) we saw a more reasonable level of diffraction efficiency on the level of about 50-60% of the total beam power (Figure 12). Seeing as this result was much more satisfactory, we moved onto testing the multiplexed AOM setup.

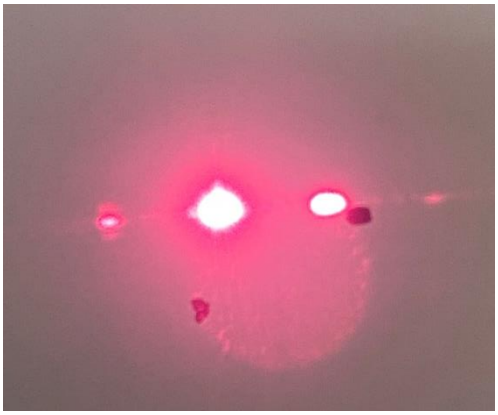

Figure 12: The beam spots from our first successful test of an AOM using the Titanium:sapphire laser (order: -1, 0^{th}, +1).

In order to test the multiplexing of the AOMs, we had to implement the multiplexing RF setup described in the previous section. After implementing this circuit for a single AOM (by removing the final splitter and decreasing the power level by 50%) we then used it to send an additive signal to the single AOM and subsequently shined the Titanium:Sapphire beam tuned to 790nm through it. As a result, we could clearly see that both the zeroth order and first order modes were diffracted into two clearly visible separate modes, with slight intermodulation modes between (Figure 13). Upon first inspection, it did not seem as though the intermodulation modes were strong enough to interfere with the diffracted modes, as was a principal concern. This provided sufficient motivation to move on to the next phase of the experiment, which involved setting up a double-pass system with two multiplexed AOMs: the final design of the interferometer.

Figure 13: The beam spots from our first successful multiplexed AOM test, with the +1 diffracted modes on the left and the 0th modes on the right.

To test the multiplexed double-pass design, we setup two multiplexed AOMs and aligned them so that the -1st order mode of the first AOM lined up with the Bragg angle of the second AOM when the multiplexed signal was unmodulated (i.e., when the signal frequencies were both 80MHz). The second AOM was then aligned so that the maximum efficiency into the +1st order mode was achieved. This led to the intended design in which the two equivalent signals cancel out the diffraction of the input beam and cause it to come out parallel to the input direction. Following this, a mirror was placed in front of the 2nd AOM so that its output was retroreflected back through the AOM system. In order to recover the subsequent collinear beam, we placed a polarizing beam splitter (PBS) upstream of the pulseshaper, and a quarter-waveplate at the entrance of the pulseshaper, so that as the light passes through the AOMs and then gets retroreflected, it gets diffracted into a different direction by the PBS (Figures 14 & 15). This design takes inspiration from the double-pass AOM system described by Donley, Heavner, et al. [20]. The result of this test was that we produced a faint, yet clearly visible on an IR reading

card, output in which the diffracted and undiffracted modes were clearly separated, and the diffracted modes formed a nearly collinear pulsetrain (Figure 16).

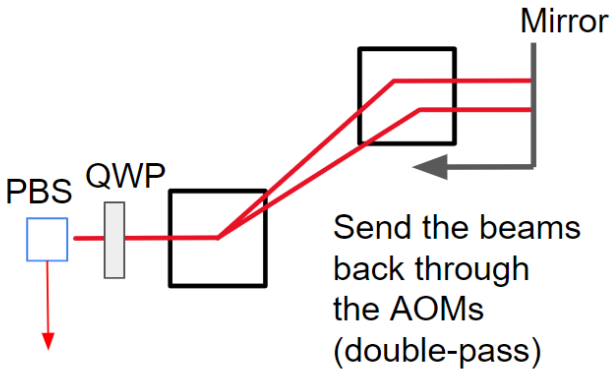

Figure 14: The finalized double-pass multiplexed AOM MZI design with a quarter-waveplate (QWP) and polarizing beam splitter (PBS).

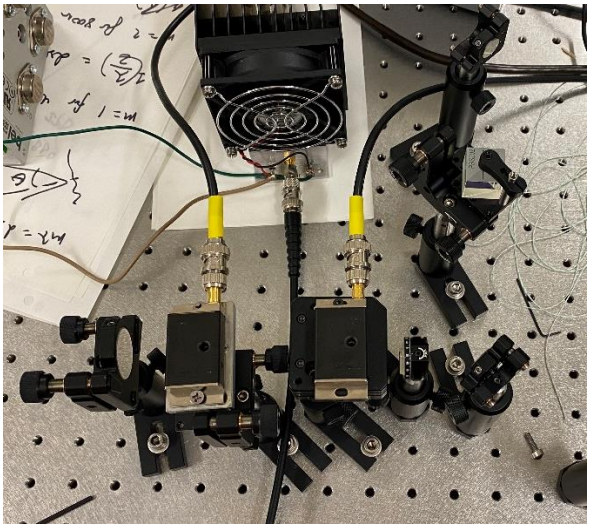

Figure 15: A picture of the double-pass multiplexed AOM MZI setup on the optical table.

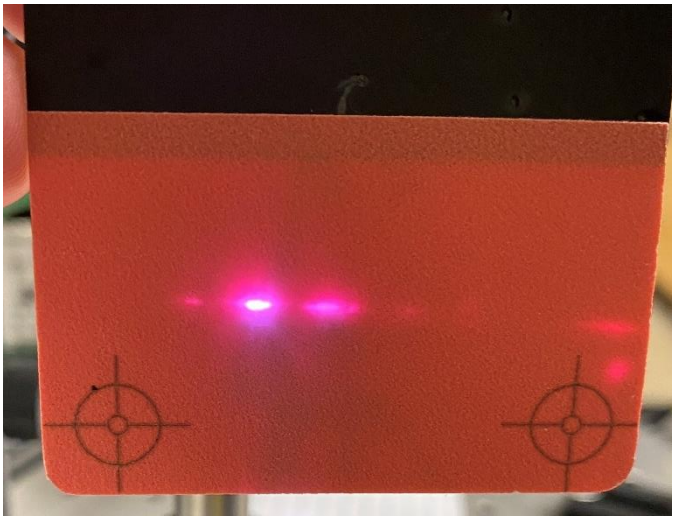

Figure 16: The beam spots produced by the AOM MZI shown previously, with the diffracted modes on the left.

We then blocked out the undiffracted modes and measured the power of the diffracted modes to determine the diffraction efficiency of the entire design based on the difference in modulation frequency of the RF signal. The results of this measure can be seen in figure 17, and we found that over a range of frequency differences from 0-40MHz, the diffraction efficiency drops from 6%-1%. While this efficiency may seem low, this result was satisfying based on the fact that we expected a much lower efficiency after moving through the AOMs four times[19], and also this frequency range is much large than we expected to use. As such, it was finally time to move on to assembling the nonlinear detection system necessary to measure the interference produced by the diffracted modes, and ultimately confirm the viability of our design.

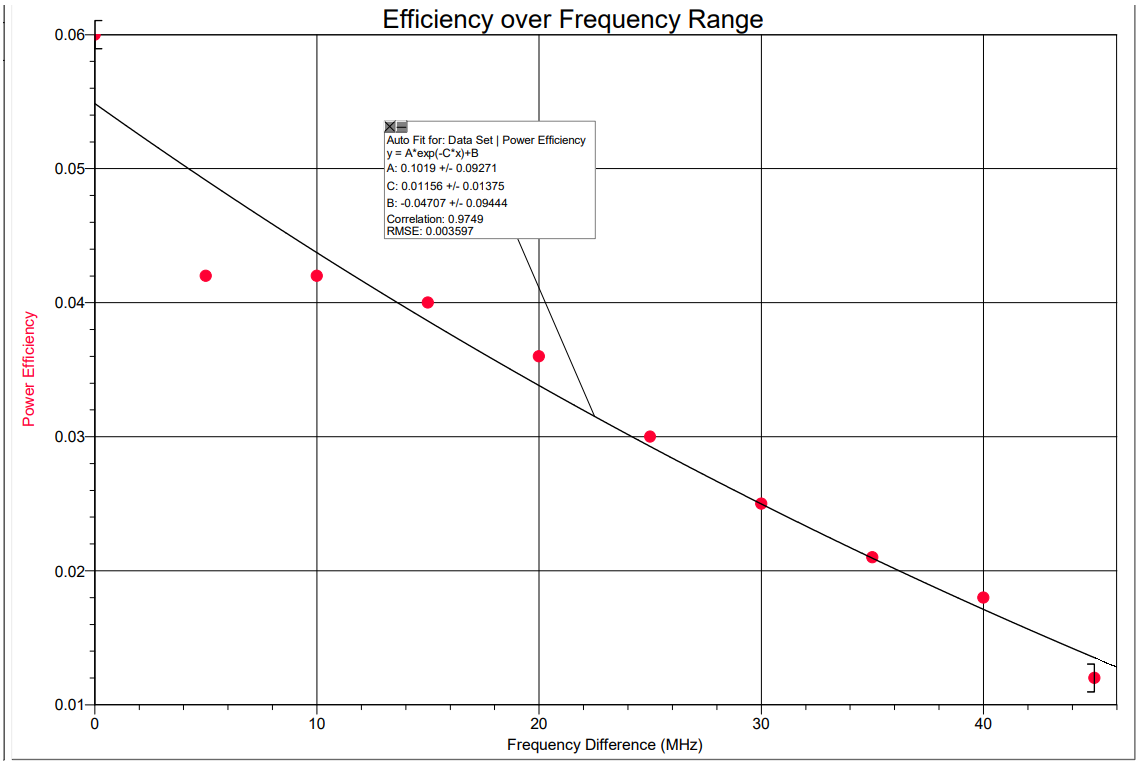

Figure 17: A graph of the diffracted modes power efficiency vs the difference in frequencies produced by the DDS channels.

C. Nonlinear 2-photon Absorption and Lock-in Amplification

To perform any experiment with a pulsed laser system, it is necessary to first characterize the pulse(s) that are used, in order to ensure that the portion of an experiment that is generating a series of carefully controlled laser pulses is actually understood and can be controlled as intended; otherwise, any observation of physical phenomena excited with these pulse(s) is inherently suspect [25]. To characterize our pulse train, we decided to use signals generated by interfering our tailored pulse train with a tracer pulse that can be delayed in time using a second, stage-based interferometer. We measured nonlinear processes based on two-photon interactions in nonlinear crystals and semiconductor heterostructures as described by the work of Hardin, Mills, et al. [18]. In general, we

planned on detecting 2-photon absorption, which occurs when an ultrafast laser is used to excite a material. If the duration of the laser pulse is sufficiently short (such as the femtosecond pulse produced by the Titanium:sapphire laser), the peak optical power is sufficient to drive nonlinear excitations, like the parametric generation of second-harmonic light in a Beta-Barium Oxide crystal. In other words, it is possible to drive excitation in a material that usually requires a beam around 400nm using an 800nm ultrafast beam. Since the ti:sapph laser is capable of generating intense laser pulses – the peak power of a femtosecond pulse from the laser has the same power as a high-performance muscle car (albeit only for a duration of 50-75 x 10^-15 seconds) focused into a spot only ~10-50um across, we decided to use devices for our detection system that exploited this, meaning we could make precise measurements of the interference effects produced by our interferometer design. This included using off-the-shelf photodiodes that detect wavelengths around 400nm but are effectively non-responsive to our fundamental at 800nm, as well as nonlinear BBO crystals capable of producing a second harmonic of the input beam [24]. In our first attempt to use this detection system, we passed the resultant diffracted pulsetrain from our AOM interferometer through a convex lens to focus it onto the BBO crystal (Figure 18). We were then able to align the crystal such that it produced a blue second-harmonic beam from the incident beam (Figures 19 & 20). We then attempted to separate the red and blue beams using a prism and measure the intensity of the second harmonic based on the RF signal modulation, but these results were inconclusive. We couldn't determine if we were measuring a second harmonic due to the constructive interference of the diffracted pulses or simply because of the two beams passing through the crystal separately. To resolve this issue and conclusively

determine if our design yielded a precise delay between the pulses, we decided to setup a separate probe beam to precisely measure the delay using our nonlinear detection system.

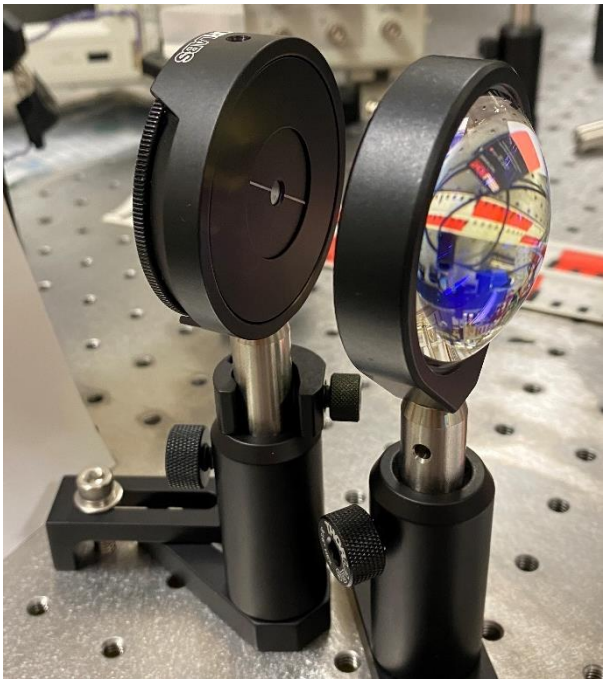

Figure 18: Convex lens focusing the pulseshaper output into the nonlinear BBO crystal.

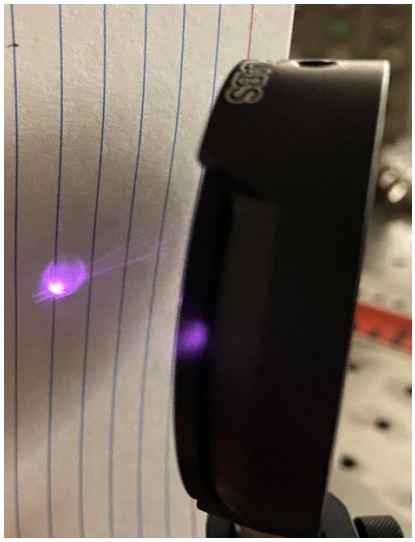

Figure 19: The red spot produced by the BBO crystal.

Figure 20: The faint second harmonic spot with the red light filtered out.

D. Precise Delay Measurement

To measure the delay created between the collinear pulses from our AOM pulseshaper, we are using a second probe pulse to create interference with the pulsetrain. In other words, we are using a beam splitter to split the original Titanium:sapphire beam near the source, and running this beam through a path that is roughly equal to the path traversed by the pulse shaped beam. On this path we have included a translation stage with a retroreflecting cornercube to precisely adjust this path length relative to the other beam. We note that this design is meant to avoid the use of precise translation stages, but this step is only necessary as a proof of concept for this design and not for the implementation of this tool. Regardless, we then sent this beam parallel with the pulseshaper output beam into the convex lens and focused it into the nonlinear crystal (Figure 21). Ideally, when the probe pulse is aligned exactly with the path lengths of the two delayed pulses, we should see constructive interference within the crystal and therefore a spike in intensity of the second harmonic generation. The efforts to precisely characterize the pulse trains generated by our novel pulse shaper are still a work in progress. To date, we have been able to observe interference between the tracer pulse and a train generated by the AOM-based device, but do not yet have a complete understanding of some incongruities we have observe (in particular, after re-building the AOM pulse shaper, we appear to be now sending the incorrect output mode to the diagnostic, and need to disassemble the device and inspect the rays produced at each step of the multi-diffraction process. By measuring

the delay between the constructive interference of the probe pulse, we should be able to directly calculate the delay between the pulses from the interferometer. This will give us a satisfactory result for the viability of this design.

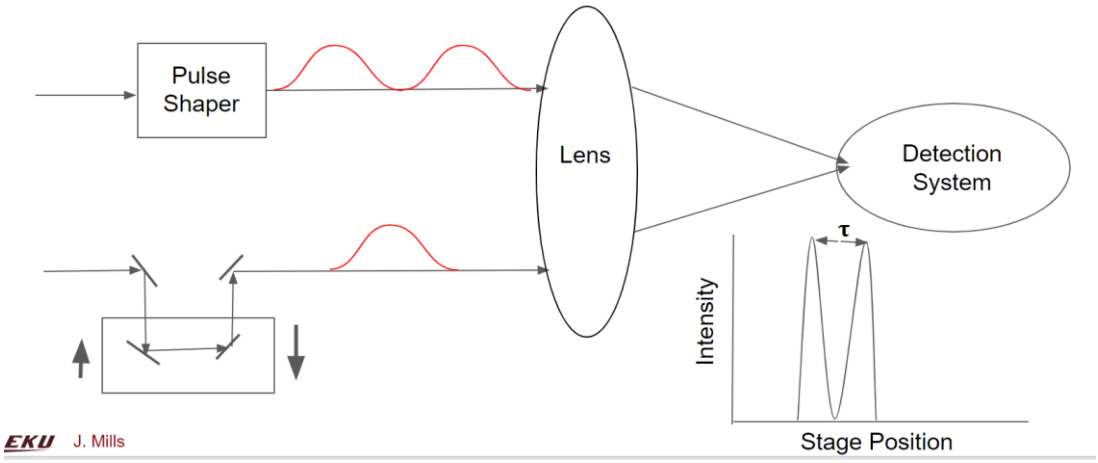

Figure 21: A diagram showing the setup of the probe pulse method for measuring the delay created by the AOM pulseshaper.

III. Conclusions

While the evaluation of this design is still a work in progress, our results thus far have shed a promising light on its viability as an optical tool. To address our initial concerns, we have found that with the double-pass multiplexed AOM design, we still recover a usable amount of power in the output beam. Additionally, it seems as though we can recover the resolution of the modes of interest without worrying about the intermodulation modes. However, these positive outcomes do not form a conclusive result. In order to conclusively state the viability of our design, we must use the previously described probe pulse method to precisely measure the delay created between the output pulses. With nonlinear detection methods resolved through lock-in signal processing, we should be able to produce a signal that will clearly show what the

interferometer is doing. The results of these tests, as well as the final decision regarding this design, will be outlined in a future publication.

References

[1]: Hecht, Eugene. "Optics 2nd edition." Optics 2nd edition by Eugene Hecht Reading (1987).

[2]: Steck, Daniel A. "Classical and modern optics." Oregon University (2006).

[3]: P. Hariharan. . Basics of Interferometry: 2nd ed. Academic Press. (2007).

[4]: Zetie, K. P.; Adams, S. F.; Tocknell, R. M. "How does a Mach–Zehnder interferometer work?". Physics Department, Westminster School, London.

[4]:

[5]: Luca Pezzé, Augusto Smerzi. “Phase sensitivity of a Mach-Zehnder interferometer”. Phys. Rev. A 73, 011801(R). (2006).

[6]: Jarvis, Thomas W. "Multiplexing acousto-optic modulators to steer polychromatic laser beams." JOSA B 32, no. 1 (2015): 83-91.

[7]: Jarvis, Thomas William. Novel tools for ultrafast spectroscopy. The University of Texas at Austin, 2011.

[8]: Jarvis, Thomas W. "Extending lock-in methods: term isolation detection of nonlinear signals." Applied optics 55, no. 22 (2016): 5846-5854.

[9]: Jarvis, Thomas W. "Isolation of weak four-wave mixing signal components in reflection experiments." IEEE Journal of Quantum Electronics 52, no. 11 (2016): 1-8.

[10]: Debye, P., and F. W. Sears. "On the scattering of light by supersonic waves." Proceedings of the National Academy of Sciences of the United States of America 18, no. 6 (1932): 409.

[11]: Bragg, William Henry, and William Lawrence Bragg. "The reflection of X-rays by crystals." Proceedings of the Royal Society of London. Series A, Containing Papers of a Mathematical and Physical Character 88, no. 605 (1913): 428-438.

[12]: Bragg, William Lawrence. "The diffraction of short electromagnetic waves by a crystal." Scientia 23, no. 45 (1929).

[13]: Korpel, Adrianus. "Acousto-optics—a review of fundamentals." Proceedings of the IEEE 69, no. 1 (1981): 48-53.

[14]: Analog Devices, Inc. Fundamentals of direct digital synthesis (dds) mt-085 tutorial rev.0. Technical report, Analog Devices, Inc., 10 2008.

[15]: Analog Devices “Mixer and Modulators,” MT-080 Tutorial.

[16]: Digi-key “The Fundamentals of RF Power Dividers and Combiners.” Art Pini. (2019).

[17]: Britannica, The Editors of Encyclopaedia. "Keplerian telescope". Encyclopedia Britannica, 8 Mar. 2019.

[18]: Wesley D. Hardin, Jon. T. Mills, Joseph M. Stuart, Eian B. Sulfridge, Tyler A. Tanner & Thomas W. Jarvis (2022) Femtosecond excitation of two-photon absorption in ruby, Spectroscopy Letters, 55:9, 552-565, DOI: 10.1080/00387010.2022.2123000

[19]: B. Fröhlich, T. Lahaye, B. Kaltenhäuser, H. Kübler, S. Müller, T. Koch, M. Fattori, and T. Pfau , "Two-frequency acousto-optic modulator driver to improve the beam pointing stability during intensity ramps", Review of Scientific Instruments 78, 043101 (2007).

[20]: E. A. Donley, T. P. Heavner, F. Levi, M. O. Tataw, and S. R. Jefferts , "Double-pass acousto-optic modulator system", Review of Scientific Instruments 76, 063112 (2005).

[21]: Interference. (n.d.). Retrieved November 16, 2022, from http://labman.phys.utk.edu/phys222core/modules/m9/interference.html

[22]: Britannica, The Editors of Encyclopaedia. "Bragg law". Encyclopedia Britannica, 15 Mar. 2022, https://www.britannica.com/science/Bragg-law. Accessed 16 November 2022.

[23]: ISOMET CORP Acousto-Optic Modulation. Application Note, AN0510.

[24]: Fritz, Amy. “Frequency Doubling in a KDP Crystal”. (2011).

[25]: Trebino, R. Frequency-Resolved Optical Gating: The Measurement of Ultrashort Laser Pulses; Springer Science & Business Media, 2012.